Acta Cryst. (1999). A**55**, 729–738

Molecular fragment electric moments derived from the fit of the experimental electrostatic potential. Application to the water molecule

Nouzha Bouhmaida,[a,b] Nour Eddine Ghermani,[a]* Claude Lecomte[a] and Abdelmalek Thalal[b]

[a]*Laboratoire de Cristallographie et Modélisation des Matériaux Minéraux et Biologiques, LCM³B, UPRES A CNRS 7036, Université Henri Poincaré, Nancy 1, Faculté des Sciences, Boulevard des Aiguillettes, BP 239, 54506 Vandoeuvre-lès-Nancy CEDEX, France, and* [b]*Laboratoire des Sciences des Matériaux, LSM, Université Cadi Ayyad, Faculté des Sciences Semlalia, Boulevard Prince Moulay Abdallah, BP S15, 40000 Marrakech, Morocco. E-mail: ghermani@lcm3b.u-nancy.fr*

(*Received 9 November 1998; accepted 13 January 1999*)

Abstract

The electrostatic potential is a multicenter property that can be expressed as a sum of the contributions of electric moments located at each atomic site of a molecule. Independently of the model used to generate the electrostatic potential around the system, these atomic moments can be accurately obtained by the fit of this physical property outside the van der Waals envelop. However, the larger the system, the greater the number of parameters. In this study a way is proposed to reduce the number of centers in the representation of the electrostatic potential which becomes a sum of fragment contributions rather than atomic ones. A sample of six water molecules in different crystal environments was chosen to discuss the derived values of the electric moments referred to the molecular center of mass.

1. Introduction

In molecular modeling and drug design, it is necessary to estimate accurately the electrostatic energy which is often predominant in the interaction between molecules. With the increase of the size of the system (polypeptides, macromolecules, proteins *etc.*), the electrostatic energy estimation is reduced, in a first approximation, to the Coulombic interaction evaluation involving the atomic net charges only. Moreover, these latter quantities are supposed to be intrinsic properties in the sense that they have to mimic the interaction of the molecule in different circumstances, that is to say, they must be ideally non-conformation-dependent. First theoretical methods to derive the net atomic charges were based on the knowledge of the electron-density distribution of the molecule. Methods like Mulliken population analysis (Mulliken, 1955) have been widely used to estimate partial atomic charges from *ab initio* theoretical calculations. These atomic charges are, however, not invariant and strictly depend on the size of the basis set used for molecular wave-function calculations. The main difficulty in deriving these atomic net charges originates from the overlapping of the electron density and from the charge transfer inside the molecule. Thus, it is necessary to partition the molecule in order to integrate the electron density in the real space of each atom to get its partial charge. Among the partitioning methods, that based on electron-density topology (Bader & Essen, 1984; Bader *et al.*, 1984; Bader, 1990) delimits the atomic space in the molecule by the zero-flux electron-density-gradient surface giving rise to nontrivial volume shapes. Another method to derive atomic net charges was proposed by Momany (1978) and is based on the molecular electrostatic potential. This observable physical property is directly related to the interaction concept since it corresponds to the electrostatic energy of a probe unit positive charge gravitating around the molecule. With respect to the electron-density integration approach, the molecular electrostatic potential possesses the advantage of being less dependent on the basis sets and it also compares very well with that derived from high-resolution X-ray diffraction (Espinosa, Lecomte, Ghermani *et al.*, 1996). In a first approximation, the molecular electrostatic potential can be described by point charges at the atomic nuclei without any volumic consideration (Gauss theorem). These charges are obtained from the molecular electrostatic potential by means of a least-squares fit. For this purpose, at each point of a sampling grid chosen around the molecule, the electrostatic potential is evaluated by quantum-mechanics calculations or from experimental results. As shown by many authors (Woods *et al.*, 1990; Ghermani *et al.*, 1993; Spackman, 1996), the grid-points location is crucial in the determination of the net charges. Different sampling points around the molecule were chosen in order to improve the fit, from cubic (Momany, 1978) to randomly distributed grid points (Woods *et al.*, 1990) on shells that are at van der Waals distances from the nuclei. Spackman (1996) has proposed a geodesic tessellation of the atomic spherical shells. We also proposed a sampling

ISSN 0108-7673

of equi-distributed points on spheres around the atoms where the contribution to the electrostatic potential on the grid points (Bouhmaida *et al.*, 1997) is weighted with respect to steric considerations. All these sampling methods joined to robust least-squares procedures were developed in order to ensure the stability of the net charge values whatever the molecular conformation and geometry.

On the other hand, Price *et al.* (1984) have shown that a truncation of the electrostatic potential at the monopole level (charge) on each nuclear site is insufficient for an accurate determination of the interaction energy. This is in agreement with Spackman (1986), who emphasized that moments up to quadrupoles are needed in the interaction energy estimation. More recently, Koch & Egert (1995) have also shown the necessity to take into account the atomic quadrupole–quadrupole interactions in force-field calculations on molecules displaying hydrogen bonds or π–π overlap. This fact is related to the difficult description of the electron deformation density by a single point charge on the atomic position for such systems. For example, interactions like the hydrogen bond involving acceptor lone pairs or like aromatic rings π–π overlap occur in the proximity of the molecules where contributions dominate those of point charges. It is also in agreement with some of our results (Ghermani *et al.*, 1993; Bouhmaida *et al.*, 1997), where we have demonstrated the experimental electrostatic potential fit improvement when the contribution from higher multipoles is taken into account; in our last paper (Bouhmaida *et al.*, 1997), we fitted the electrostatic potential with a set of net charges and multipole moments centered at each nucleus which accurately describes the experimental electrostatic potential. Even though the number of multipole moments has been reduced by chemical constraint or statistical consideration, it remains high (132 parameters for a 30-atom molecule) to be used directly in force-field calculations for large systems. Therefore, in this paper, we propose a method to recover the molecular electrostatic potential from fragmental rather than atomic contributions: we have used the analytical transformations of the real spherical harmonics (Hobson, 1931) in order to evaluate the Buckingham electric moments (Buckingham, 1959) for chosen fragments of a molecule after an initial fit of the electrostatic potential which provides the moments for each atom of the system (Bouhmaida *et al.*, 1997). This method may be applied to electrostatic potentials obtained from other experiments or theoretical calculations. Without any integration of the electron density, the results allow retrieval of intrinsic physical properties of the fragments which can be compared with theoretical calculations or experimental measurements (*e.g.* dielectric permittivity, Stark effect, induced birefringence). This paper describes the method and shows applications to the water molecule.

2. Methodology

2.1. *Molecular-fragment moments from the fit of the experimental electrostatic potential*

In the Hansen–Coppens model (Hansen & Coppens, 1978) used for the determination of the electron density from high-resolution X-ray diffraction data, the pseudo-atom electron density is given by

$$\rho_{\rm at}(\mathbf{r}) = \rho_{\rm core}(r) + P_{\rm val}\kappa^3\rho_{\rm val}(\kappa r) + \sum_l \kappa'^3 R_{nl}(\kappa' r)\sum_m P_{lm} y_{lm\pm}(\theta,\varphi), \qquad (1)$$

where $\rho_{\rm core}(r)$ and $\rho_{\rm val}(r)$ are the spherical core and valence Hartree–Fock electron densities, respectively. $y_{lm\pm}$ are the real spherical harmonics modulated by the Slater-type radial functions $R_{nl}(r)$. $P_{\rm val}$ and P_{lm} are the valence and the deformation populations and κ and κ' are electronic cloud contraction–expansion coefficients (Coppens *et al.*, 1979).

Once these model parameters are determined, the molecular electrostatic potential can be calculated analytically (Ghermani *et al.*, 1991, 1992–1998) and taken as observable to fit the atomic net charges (Ghermani *et al.*, 1993) and atomic multipolar moments (Bouhmaida *et al.*, 1997) using the expansion:

$$V(\mathbf{r}) = \sum_j \sum_{lm} Q_{jlm} y_{lm\pm}(\theta,\varphi)/|\mathbf{r}-\mathbf{R}_j|^{l+1}, \qquad (2)$$

where Q_{jlm} is the nucleus-centered fitted lth-order moment of atom j at $\mathbf{R}_j$, θ and φ are the spherical angles of the vector $(\mathbf{r}-\mathbf{R}_j)$ and $y_{lm\pm}$ are the angular functions defined in Appendix *A*. In our fitting procedure (Bouhmaida *et al.*, 1997), the sampling points are equi-distributed on spherical shells around each nucleus (Ghermani *et al.*, 1993). The originality of our method lies in the cancellation of the jth-atom contribution to the electrostatic potential when its distance $|\mathbf{r}-\mathbf{R}_j|$ to the grid point is less than 2 Å. The fitted Q_{jlm} atomic multipole moments are given in the local atomic frame, which allows comparison between chemically constrained or symmetry-equivalent atoms.

In order to formulate the total moment for a given fragment, it is necessary to express the fitted atomic moments with respect to a common origin $\mathbf{R}_g$ chosen for example at the center of mass of this fragment. Using the definition of the spherical harmonics, formula (2) can be rewritten:

$$V(\mathbf{r}) = \sum_j \sum_{lm\geq 0} [N_{lm}P_l^m(\cos\theta)/|\mathbf{r}-\mathbf{R}_j|^{l+1}] \times (Q_{jlm}\cos m\varphi + Q_{jl\bar{m}}\sin m\varphi), \qquad (3)$$

where the $P_l^m(\cos\theta)$ are the associated Legendre polynomials, $\bar{m} = -m$ and N_{lm} are the normalization factors given in Appendix *A*. A positive translation $c = |\mathbf{R}_g - \mathbf{R}_j|$, where $\mathbf{R}_j$ is the nucleus center, parallel to the k axis leaves the φ angle of vector $(\mathbf{r}-\mathbf{R}_j)$ unmodified where θ changes to θ' (see Fig. 1). With

respect to this k-axis translation, we have $|\mathbf{r}-\mathbf{R}_j|\cos\theta = |\mathbf{r}-\mathbf{R}_g|\cos\theta' + c$ and, when $c < |\mathbf{r}-\mathbf{R}_g|$, the Legendre polynomials $P_l^m(\cos\theta)$ related to angle θ become (Hobson, 1931):

$$\begin{aligned}P_l^m(\cos\theta)/|\mathbf{r}-\mathbf{R}_j|^{l+1} &= P_l^m(\cos\theta')/|\mathbf{r}-\mathbf{R}_g|^{l+1} - c(l-m+1)\\ &\times P_{l+1}^m(\cos\theta')/|\mathbf{r}-\mathbf{R}_g|^{l+2} + \frac{1}{2!}c^2(l-m+1)\\ &\times (l-m+2)P_{l+2}^m(\cos\theta')/|\mathbf{r}-\mathbf{R}_g|^{l+3}\\ &- \frac{1}{3!}c^3(l-m+1)(l-m+2)(l-m+3)\\ &\times P_{l+3}^m(\cos\theta')/|\mathbf{r}-\mathbf{R}_g|^{l+4} + \ldots, \end{aligned} \tag{4}$$

where $\cos\theta$ and $\cos\theta'$ are polar coordinates of $(\mathbf{r}-\mathbf{R}_j)$ and $(\mathbf{r}-\mathbf{R}_g)$ vectors, respectively. Then, the translated j-atom moment Q'_{jlm} with respect to the new origin at $\mathbf{R}_g$ (center of mass) is related to nucleus-centered moments Q_{jlm} as follows:

$$Q'_{jlm} = \sum_{k\geq|m|}^{l} (-1)^{l-k}[(l-|m|)!/(l-k)!(k-|m|)!]c^{l-k}Q_{jkm}. \tag{5}$$

Q'_{jlm} moment expressions for $l=1$ to $l=4$ are listed in Appendix B. These relations are in good agreement with those given by McLean & Yoshimine (1967) in their paper dealing with the transformation of components of the polarization tensors. It is worth noting that the charges and the atomic moments $Q_{jl(\pm l)}$, which are not θ dependent, are invariant in this origin translation. Once this translation is made, the molecular fragment moments are then obtained by summing the corresponding translated atomic moments.

2.2. *Molecular fragment traceless moments*

The electrostatic potential expansion is originally related to the traceless moments (Buckingham, 1959):

$$\begin{aligned}V(\mathbf{r}) = Q/r + \sum_\alpha \mu_\alpha r_\alpha/r^3 + \sum_{\alpha\beta}(\Theta_{\alpha\beta}/3r^5)[3r_\alpha r_\beta - r^2\delta_{\alpha\beta}]\\ + \sum_{\alpha\beta\gamma}(\Omega_{\alpha\beta\gamma}/5r^7)[5r_\alpha r_\beta r_\gamma - r^2(r_\alpha\delta_{\beta\gamma} + r_\beta\delta_{\gamma\alpha}\\ + r_\gamma\delta_{\alpha\beta})] + \sum_{\alpha\beta\gamma\delta}(\Phi_{\alpha\beta\gamma\delta}/7r^9)[7r_\alpha r_\beta r_\gamma r_\delta\\ - r^2(r_\alpha r_\beta\delta_{\gamma\delta} + r_\beta r_\gamma\delta_{\alpha\delta} + r_\alpha r_\gamma\delta_{\beta\delta} + r_\alpha r_\delta\delta_{\beta\gamma}\\ + r_\beta r_\delta\delta_{\alpha\gamma} + r_\delta r_\gamma\delta_{\alpha\beta})\\ + (r^4/5)(\delta_{\alpha\beta}\delta_{\gamma\delta} + \delta_{\alpha\delta}\delta_{\beta\gamma} + \delta_{\alpha\gamma}\delta_{\beta\delta})]\ldots, \end{aligned} \tag{6}$$

where μ_α are the dipole moment components, $\Theta_{\alpha\beta}$, $\Omega_{\alpha\beta\gamma}$ and $\Phi_{\alpha\beta\gamma\delta}$ are the traceless quadrupole, octupole and hexadecapole moment tensors, respectively. These quantities are defined as follows:

$$\begin{aligned}\Theta_{\alpha\beta} &= \tfrac{1}{2}\int_v \rho(\mathbf{r})(3r_\alpha r_\beta - r^2\delta_{\alpha\beta})\,\mathrm{d}\mathbf{r}\\ \Omega_{\alpha\beta\gamma} &= \tfrac{1}{2}\int_v \rho(\mathbf{r})[5r_\alpha r_\beta r_\gamma - r^2(r_\alpha\delta_{\beta\gamma} + r_\beta\delta_{\gamma\alpha} + r_\gamma\delta_{\alpha\beta})]\,\mathrm{d}\mathbf{r}\\ \Phi_{\alpha\beta\gamma\delta} &= \tfrac{5}{8}\int_v \rho(\mathbf{r})[7r_\alpha r_\beta r_\gamma r_\delta - r^2(r_\alpha r_\beta\delta_{\gamma\delta} + r_\beta r_\gamma\delta_{\alpha\delta}\\ &\quad + r_\alpha r_\gamma\delta_{\beta\delta} + r_\alpha r_\delta\delta_{\beta\gamma} + r_\beta r_\delta\delta_{\alpha\gamma} + r_\delta r_\gamma\delta_{\alpha\beta})\\ &\quad + (r^4/5)(\delta_{\alpha\beta}\delta_{\delta\gamma} + \delta_{\alpha\delta}\delta_{\beta\gamma} + \delta_{\alpha\gamma}\delta_{\beta\delta})]\,\mathrm{d}\mathbf{r}, \end{aligned} \tag{7}$$

where $\rho(\mathbf{r})$ is the electron density of the molecule. The traceless conditions are $\sum_\alpha \Theta_{\alpha\alpha} = 0$, $\sum_\alpha \Omega_{\alpha\alpha\beta} = 0$, $\sum_\alpha \Phi_{\alpha\alpha\beta\delta} = 0$ for the quadrupoles, octupoles and hexadecapoles, respectively.

In our case, according to the Cartesian harmonics given in Appendix A, the expression for the electrostatic potential up to octupole level, in the case of one fragment, can be expressed as:

$$\begin{aligned}V(\mathbf{r}) = Q_{00}/|\mathbf{r}-\mathbf{R}_g| + (Q_{11}x + Q_{1\bar1}y + Q_{10}z)/|\mathbf{r}-\mathbf{R}_g|^3\\ + [Q_{22}(x^2-y^2) + Q_{2\bar2}xy + Q_{21}xz + Q_{2\bar1}yz\\ + Q_{20}(3z^2-r^2)]/|\mathbf{r}-\mathbf{R}_g|^5 + [Q_{33}(x^3-3xy^2)\\ + Q_{3\bar3}(3yx^2-y^3) + Q_{32}z(x^2-y^2) + Q_{3\bar2}xyz\\ + Q_{31}(5z^2x-r^2x)]/|\mathbf{r}-\mathbf{R}_g|^7\\ + [Q_{3\bar1}(5z^2y-r^2y) + Q_{30}(5z^3-3r^2z)]/|\mathbf{r}-\mathbf{R}_g|^7. \end{aligned} \tag{8}$$

The monopole and dipole contributions to the electrostatic potential are the same as in formula (6); in order to be in agreement with the Buckingham (1959) definition, the quadrupole and the octupole part $V_{Q,O}(\mathbf{r})$ of this potential can be reformulated as:

$$\begin{aligned}V_{Q,O}(\mathbf{r}) = |\mathbf{r}-\mathbf{R}_g|^{-5}[(Q_{22}-Q_{20})x^2 - (Q_{22}+Q_{20})y^2\\ + 2Q_{20}z^2 + Q_{2\bar2}xy + Q_{21}xz + Q_{2\bar1}zy]\\ + |\mathbf{r}-\mathbf{R}_g|^{-7}[(Q_{33}-Q_{31})x^3 - (Q_{3\bar3}+Q_{3\bar1})y^3\\ + 2Q_{30}z^3 + (3Q_{3\bar3}-Q_{3\bar1})yx^2\\ - (3Q_{33}+Q_{31})xy^2 + 4Q_{31}xz^2 + 4Q_{3\bar1}yz^2\\ + (Q_{32}-3Q_{30})zx^2 - (Q_{32}+3Q_{30})zy^2\\ + Q_{3\bar2}xyz]. \end{aligned}$$

Consequently, the relations between the fitted Q_{lm} moments and the Buckingham traceless components are:

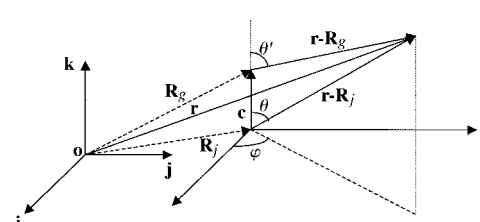

Fig. 1. Origin translation and related vectors.

Table 1. *Water molecule bond lengths (Å) and angles (°)*

The s.u.'s in parentheses for LAP are for neutron diffraction results.

	TGG	ENK	ASPA1	ASPA2	LAP	NAT
O_w-H_{w1}	0.96	0.96	0.96	0.96	0.967 (5)	0.97
O_w-H_{w2}	0.96	0.96	0.96	0.96	0.992 (5)	0.97
$H_{w1}-O_w-H_{w2}$	110.0	98.8	108.0	110.9	107.6 (4)	114.5
Water molecule bonds						
O_w	1.77 (H—N)	1.94 (H—N)	1.80 (H—O) 1.89 (H—N)	1.80 (H—O)	1.883 (5) (H—N)	2.37 (Na^+) 2.39 (Na^+)
$H_{w1}\cdots O$	1.85	1.79	1.73	1.97	1.793 (4)	1.89
$H_{w2}\cdots O$	1.79	1.89	1.75	1.80	1.847 (5)	2.06

$$
\begin{aligned}
\Theta_{xx} &= Q_{22} - Q_{20} & \Theta_{xy} &= \tfrac{1}{2}Q_{2\bar{2}} \\
\Theta_{yy} &= -Q_{22} - Q_{20} & \Theta_{xz} &= \tfrac{1}{2}Q_{21} \\
\Theta_{zz} &= 2Q_{20} & \Theta_{yz} &= \tfrac{1}{2}Q_{2\bar{1}} \\
\Omega_{xxx} &= Q_{33} - Q_{31} & \Omega_{yyx} &= -Q_{33} - Q_{31}/3 \\
\Omega_{zzx} &= \tfrac{4}{3}Q_{31} & \Omega_{xxy} &= Q_{3\bar{3}} - Q_{3\bar{1}}/3 \\
\Omega_{yyy} &= -Q_{3\bar{3}} - Q_{3\bar{1}} & \Omega_{zzy} &= \tfrac{4}{3}Q_{3\bar{1}} \\
\Omega_{xxz} &= -Q_{30} + Q_{32}/3 & \Omega_{yyz} &= -Q_{30} - Q_{32}/3 \\
\Omega_{zzz} &= 2Q_{30} & \Omega_{xyz} &= \Omega_{3\bar{2}}/6.
\end{aligned}
\tag{9}
$$

Furthermore, the symmetric traceless quadrupole tensor can be diagonalized to get the eigenvalues and the eigenvectors of the quadrupole moment.

All these transformations are coded in a new version of the *ELECTROS* program (Ghermani *et al.*, 1992–1998), which determines the atomic moments using the fit of the electrostatic potential. The calculations of molecular or fragmental moments are performed in the center-of-mass local frame and the obtained quadrupole traceless components are diagonalized for comparison with other experimental or theoretical results. From the least-squares method, we get the variance–covariance matrix M_x. The propagation of errors is calculated using the formula $M_u = DM_xD^T$ (Coppens, 1997), where D is the matrix of the derivatives of the new parameters u_j with respect to the variables x_i. The calculated standard uncertainties (s.u.'s) do not take into account either the variances of the experimental electrostatic potential values at the grid points or the s.u.'s of the atomic positional parameters.

3. Application to the water molecule

The water molecule has the advantage of being small and therefore numerous theoretical calculations and experimental results of molecular moments are available in the literature (see for example Colonna *et al.*, 1990; Spackman, 1992). Our six-water-molecule sample

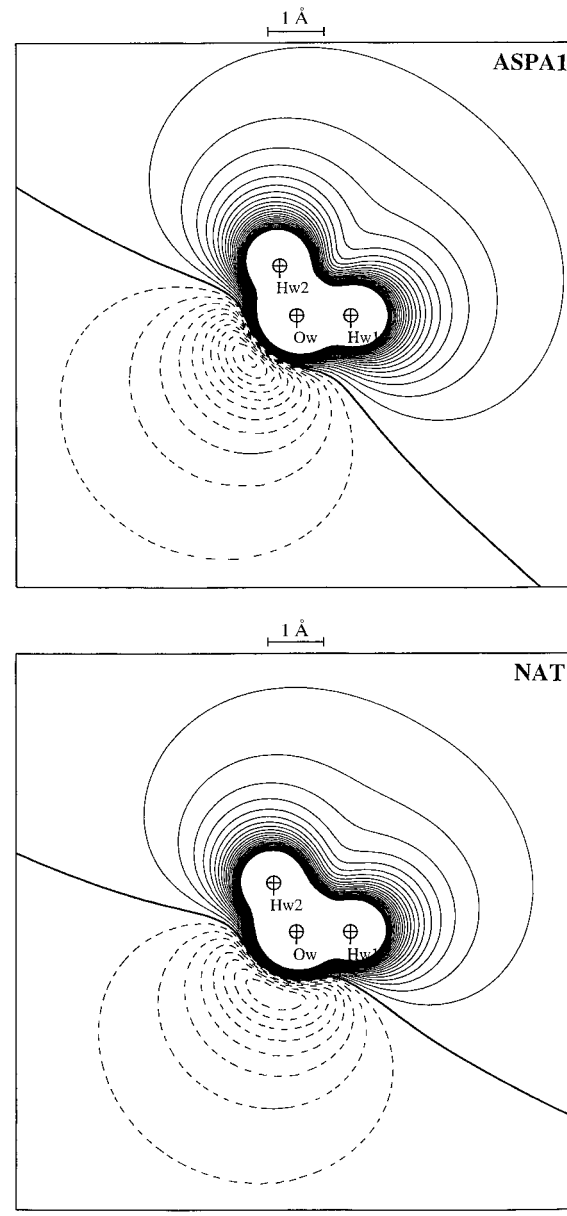

Fig. 2. Experimental electrostatic potential for ASPA1 and NAT water molecules. Contour intervals are 0.02 e $Å^{-1}$; negative contours are dashed and the zero contour is the heavy line.

Table 2. *Water molecule electric moments in the center of mass inertial frame and the averaged values of significant moments*

The least-squares standard uncertainties (s.u.'s) and the root mean square deviations for the mean values are given in parentheses.

	TGG	ENK	ASPA1	ASPA2	LAP	NAT	Averaged moments
Charge q	−0.004 (1)	−0.007 (1)	0.004 (1)	0.004 (1)	0.002 (1)	0.001 (1)	–
Dipoles (10^{-30} C m)							
μ_x	0.503 (1)	−0.597 (2)	−0.228 (1)	−0.163 (1)	0.686 (1)	0.867 (2)	–
μ_y	0.006 (1)	−0.522 (1)	1.308 (1)	0.933 (1)	−0.584 (1)	−1.823 (1)	–
μ_z	**6.494 (1)**	**8.412 (2)**	**7.949 (1)**	**7.110 (1)**	**7.413 (1)**	**6.700 (1)**	**7.3 (7)**
Modulus	**6.513 (1)**	**8.450 (2)**	**8.059 (1)**	**7.173 (1)**	**7.467 (1)**	**6.998 (1)**	**7.4 (7)**
In debye	**1.953 (1)**	**2.533 (1)**	**2.416 (1)**	**2.150 (1)**	**2.239 (1)**	**2.098 (1)**	**2.2 (2)**
Quadrupoles (10^{-40} C m^2)							
Θ_{xx}	**8.554 (4)**	**8.592 (5)**	**10.973 (5)**	**10.859 (4)**	**8.876 (4)**	**7.972 (5)**	**9.3 (13)**
Θ_{yy}	**−7.587 (3)**	**−10.542 (5)**	**−9.383 (3)**	**−10.089 (3)**	**−7.630 (3)**	**−6.186 (4)**	**−8.6 (17)**
Θ_{zz}	−0.968 (4)	1.950 (5)	−1.589 (4)	−0.770 (3)	−1.246 (4)	−1.786 (4)	–
Octupoles (10^{-50} C m^3)							
Ω_{xxx}	−0.165 (10)	−0.336 (12)	0.006 (10)	0.631 (8)	−0.163 (10)	0.769 (11)	–
Ω_{yyy}	−0.015 (9)	1.028 (12)	−1.363 (9)	1.796 (7)	1.279 (9)	2.147 (9)	–
Ω_{zzz}	**−7.101 (8)**	**−6.594 (12)**	**−6.874 (10)**	**−8.425 (7)**	**−6.446 (8)**	**−6.298 (9)**	**−6.9 (7)**
Ω_{xxy}	0.005 (7)	−0.642 (9)	1.569 (7)	−1.098 (6)	−1.060 (7)	−1.927 (8)	–
Ω_{xxz}	**11.772 (7)**	**12.973 (11)**	**12.204 (8)**	**14.907 (6)**	**10.824 (7)**	**9.843 (8)**	**12.1 (17)**
Ω_{yyx}	−0.006 (7)	0.189 (10)	0.458 (7)	−0.415 (6)	−1.336 (7)	1.364 (7)	–
Ω_{yyz}	**−4.671 (7)**	**−6.380 (10)**	**−5.330 (7)**	**−6.482 (5)**	**−4.378 (7)**	**−3.545 (7)**	**−5.1 (11)**
Ω_{zzx}	0.171 (9)	0.146 (11)	−0.519 (9)	−0.216 (7)	1.499 (9)	−2.133 (10)	–
Ω_{zzy}	0.010 (6)	−0.386 (10)	−0.206 (7)	−0.697 (5)	−0.219 (6)	−0.219 (7)	–
Ω_{xyz}	−0.009 (6)	0.270 (8)	1.714 (6)	−0.114 (5)	−0.146 (6)	0.808 (6)	–

originates from several charge-density studies; all the water molecules are hydrogen bonded to peptide or amino acid molecules: leucine–enkephaline trihydrate (hereafter ENK) (Pichon-Pesme *et al.*, 1994), tyrosine–glycine–glycine monohydrate (hereafter TGG) (Lachekar, 1997), aspartic acid–glycine dihydrate (hereafter ASPA1 and ASPA2 for the two independent water molecules) (Lachekar, 1997), L-arginine phosphate monohydrate (hereafter LAP) (Espinosa, Lecomte, Molins *et al.*, 1996); the last water molecule is bound to the framework of a natural zeolite, natrolite (hereafter NAT) (Ghermani *et al.*, 1996). Table 1 gives the bond lengths and angles of these water molecules and their respective hydrogen and oxygen bonds in the crystal based on X-ray diffraction experiments (except for LAP for which the neutron diffraction structure was used). In all X-ray diffraction experiments, H atoms were found from Fourier difference maps and their coordinates were extended along the O—H bond according to the neutron data value [d(O—H) = 0.96 Å (Allen, 1986)], therefore, the O—H bond lengths are equal. For the LAP water molecule in the crystal (neutron data), one O_w—H_w bond length is longer [0.992 (5) Å]. For the six water molecules, H_w—O_w—H_w angle values are in the range 98.8 (ENK) to 114.5° (NAT) owing to hydrogen-bond interactions. All the water-molecule O atoms are hydrogen bonded to H—O or H—N bonds except for the NAT O atom, which is coordinated to two Na^+ cations. Moreover, NAT and ASPA1 O atoms both accept two bonds ($O_w\cdots Na^+$ = 2.37 and 2.39 Å for NAT and $O_w\cdots$H—O = 1.80, $O_w\cdots$H—N = 1.89 Å for ASPA1). All the water-molecule H-atom pairs are linked to O atoms in the crystals. The shortest hydrogen-bond length is found in the ASPA1 crystal ($H_w\cdots O$ = 1.73 Å), the longest in the NAT zeolite compound ($H_w\cdots O$ = 2.06 Å).

The electron-density multipole parameters (Pichon-Pesme *et al.*, 1994; Lachekar, 1997; Espinosa, Lecomte, Molins *et al.*, 1996; Ghermani *et al.*, 1996) were used to calculate the experimental electrostatic potential for the six pseudo-isolated water molecules. As an example, Fig. 2 displays the observed electrostatic potential around NAT and ASPA1 water molecules. The maps for the other molecules have been deposited.† The effect of environment interaction shows on the extent of both positive (electrophilic) and negative (nucleophilic) regions as well as the electrostatic potential minimum at

† The observed electrostatic potential around the water molecules for TGG, ASPA2, LAP and ENK, the electric moments generated electrostatic potential up to hexadecapole level for TGG, ASPA2, ENK and LAP water molecules, the difference maps between the generated potential with moments up to hexadecapole level and the observed electrostatic potential for ASPA1 and NAT water molecules, and a table giving the hexadecapole moments for the six water molecules have been deposited with the IUCr. These are available from the IUCr electronic archives (Reference: AU0162). Services for accessing these data are described at the back of the journal.

approximately 1 Å from the O_w nuclei, which is in the range −0.14 (TGG) to −0.22 e Å^{-1} (ASPA1) for the six molecules.

In order to get the Q_{jlm} atomic moments, the fit of the electrostatic potential was carried out with 177 spherically equi-distributed grid points per atom (Ghermani *et al.*, 1993) at a distance $|\mathbf{r} - \mathbf{R}_j|$ equal to 2 Å from the nuclei using the method described in the previous paper (Bouhmaida *et al.*, 1997). The obtained least-squares residual factors defined by

$$R(\%) = \left[\sum_i^{N_{\text{obs}}} (V_{\text{obs}_i} - V_{\text{calc}_i})^2 \Big/ \sum_i^{N_{\text{obs}}} V_{\text{obs}_i}^2 \right]^{1/2}$$

are all less than 0.2% for any water molecule, showing the adequacy of the fit. These atomic moments were used to calculate the molecular moments [formula (4) in §2] with respect to an origin at the molecular center of mass as recommended by Spackman (1992). The orthonormal frame was chosen such that the *k* axis bisects the two O_w—H_w bonds, the *i* axis being in the plane of the water molecule. Table 2 gives the results for each of the six water molecules. Without any electroneutrality constraint in the fit procedure, the total charge is almost zero for all the molecules. The molecular dipole moment (in debye, 1 D = 3.33564×10^{-30} C m) values are in the range of 1.95 (TGG) to 2.53 D (ENK). Spackman (1992, and references cited therein) has reported water-molecule dipole-moment magnitudes ranging from 1.6 to 2.7 D from X-ray diffraction experiments, 1.9 D from gas measurement and 2.2 D from SCF/6-31G** theoretical calculations. These values are in excellent agreement with those derived in the present study from the fit of electrostatic potential given in Table 2.

In our study, the calculated mean dipole moment value is equal to 2.23 D with an estimated root mean square deviation σ_{n-1} = 0.22 D for the chosen six-molecule sample. This dispersion certainly reflects the different environments of the water molecules in the solid state. Furthermore, the very low standard uncertainties (s.u.'s) given in Table 2 are solely derived from the least-squares method and are far from this σ_{n-1} value. On the other hand, the dipole moment for a free

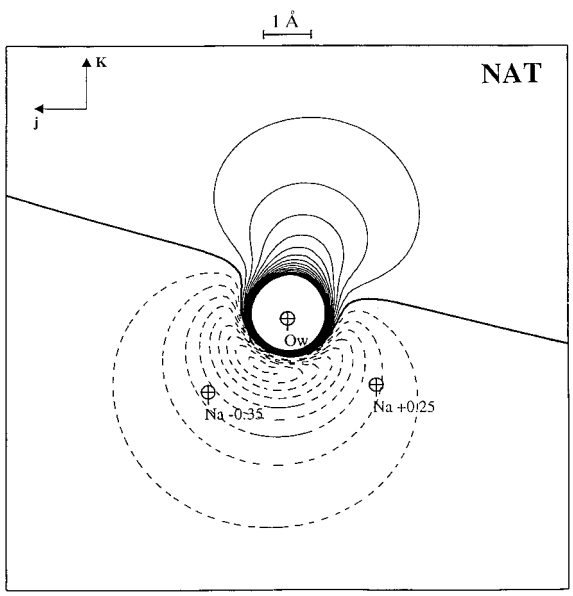

Fig. 3. Experimental electrostatic potential for NAT water molecule in the *jk* plane. The distance to the plane of the Na^+ cation neighbors is indicated close to the label. Same contours as in Fig. 2.

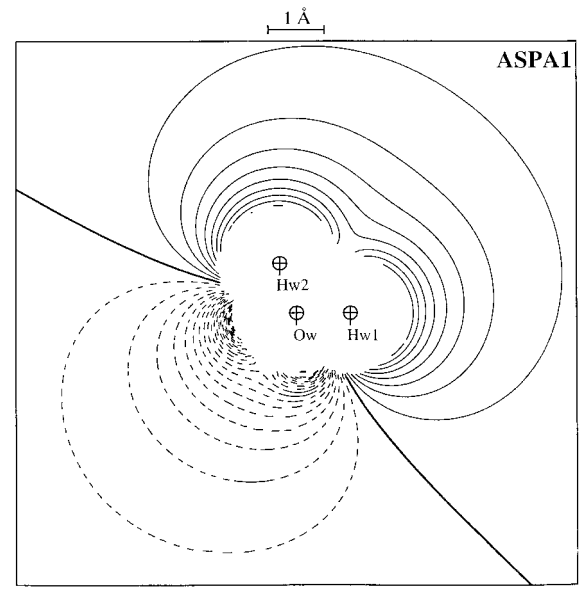

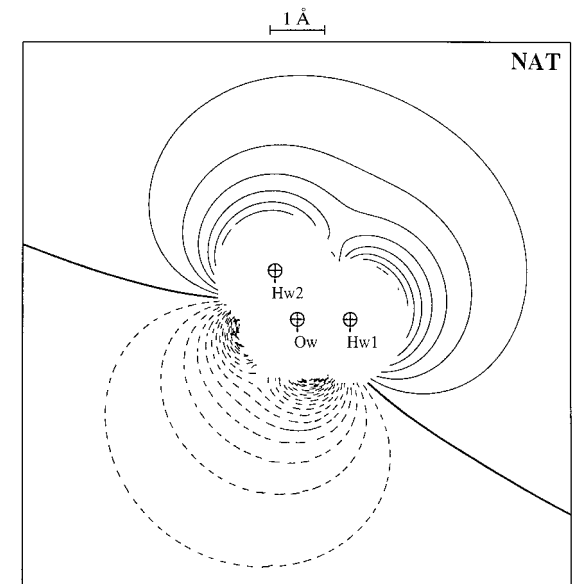

Fig. 4. Up to octupole level electric moments generated electrostatic potential for ASPA1 and NAT water molecules. Same contours as in Fig. 2.

water molecule must be ideally parallel to the chosen k axis respecting C_{2v} symmetry. However, owing to intermolecular interactions in the crystal, ASPA1 and NAT water molecules have non-negligible dipole components along the j axis perpendicular to the molecular plane, the higher value of μ_y reaching 0.55 D for the NAT molecule. According to their environment in the solid state, ASPA1 and NAT are those that have a doubly bonded O atom. The molecule dipole-moment vector component along the j axis may be related to O_w lone-pair rotation owing to the asymmetric $O_w \cdots X$ bonds as shown in Fig. 3, which displays the electrostatic potential around the NAT water molecule in the jk plane. On the other hand, a nonzero μ_x molecular dipole component involves the contribution of both O and H atoms. The largest μ_x value of 0.26 D [0.867 (2) $\times 10^{-30}$ C m] was found for the NAT water molecule. In Table 2 are also given the eigenvalues of the traceless quadrupole moment tensor with respect to the center-of-mass inertial frame. The obtained values are of the same order of magnitude as those reported by Spackman (1992) from experimental (for the gas, $\theta_{xx} = 8.77$, $\theta_{yy} = -8.34$ and $\theta_{zz} = -0.43 \times 10^{-40}$ C m^2; from multipole analysis, $\theta_{xx} = 11.0$, $\theta_{yy} = -13.0$ and $\theta_{zz} = 2.0 \times 10^{-40}$ C m^2) or theoretical estimates (*ab initio* SCF/6-31G**, $\theta_{xx} = 7.93$, $\theta_{yy} = -7.59$ and $\theta_{zz} = -0.33 \times 10^{-40}$ C m^2). For all water molecules, the eigenvectors, *i.e.* the principal directions of the quadrupole tensor, are nearly parallel to the reference axes. The θ_{xx} and θ_{yy} components have comparable absolute values between 7.5 and 11.0×10^{-40} C m^2, respectively, when θ_{zz} is on average at least three times lower. The θ_{zz} sign is negative for all the molecules except ENK, for which the corresponding absolute value of this component is also the highest. In the leucine–enkephaline (ENK) study, owing to the great number of atoms in the unit cell, the three water molecules were constrained during the electron-density refinement (Pichon-Pesme *et al.*, 1994). Therefore, the obtained values have to be considered with caution. Three significant Ω octupole moment tensor principal components arise from the fit of the experimental electrostatic potential for the six water molecules: Ω_{zzz}, Ω_{xxz} and Ω_{yyz} with on average $|\Omega_{xxz}| > |\Omega_{zzz}| > |\Omega_{yyz}|$ (Table 2). The respective values of the principal octupole components compare well from one molecule to another. Comparatively, if the magnitude of the water-molecule quadrupole-moment components agree with those reported by Colonna *et al.* (1990) [SCF wavefunction calculation using distributed multipole analysis

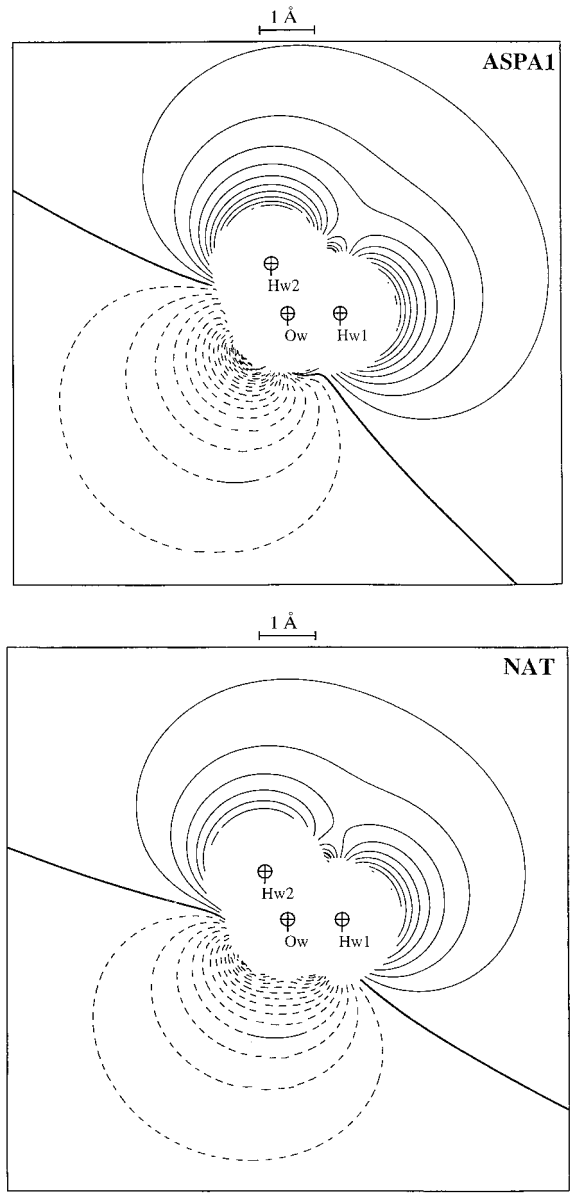

Fig. 5. Up to hexadecapole level electric moments generated electrostatic potential for ASPA1 and NAT water molecules. Same contours as in Fig. 2.

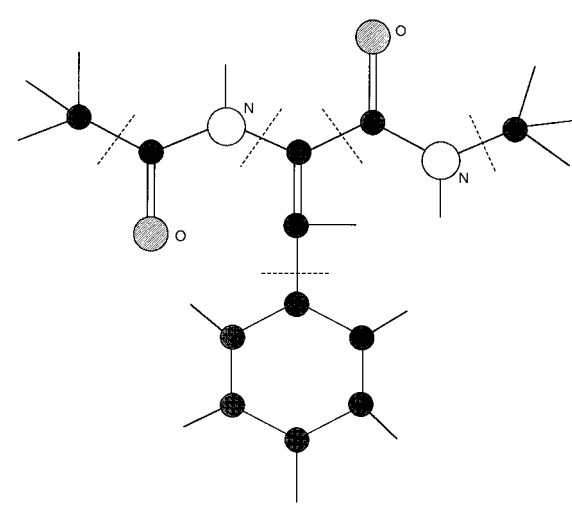

Fig. 6. The six chosen fragments of the pseudopeptide molecule *N*-acetyl-α,β-dehydrophenylalanine methylamide (broken lines).

(DMA)], their octupole components are about two times lower than those obtained in the present study.

The electrostatic potential calculated with the molecular moments reported in Table 2 is shown in Fig. 4 for NAT and ASPA1 water molecules. The calculated and observed electrostatic potential (Fig. 2) features compare very well beyond a distance of 1.5 Å from the nuclear sites. However, two negative lobes appear at a close distance from the O_w nucleus on both maps in Fig. 4. They are due to the limitation at the octupole level of the molecular moment at the center of mass; the reduction from three centers to one center necessitates higher multipole functions. To show this, we have calculated corresponding hexadecapole moments at the center of mass using (4), from the O_w and H_w atomic moments (octupole level for O_w and dipole level for H_w). The correspondence between Q_{lm} moments and the Buckingham traceless hexadecapole components are given in Appendix *C*. The values of the hexadecapole moments for the six water molecules have been depos-

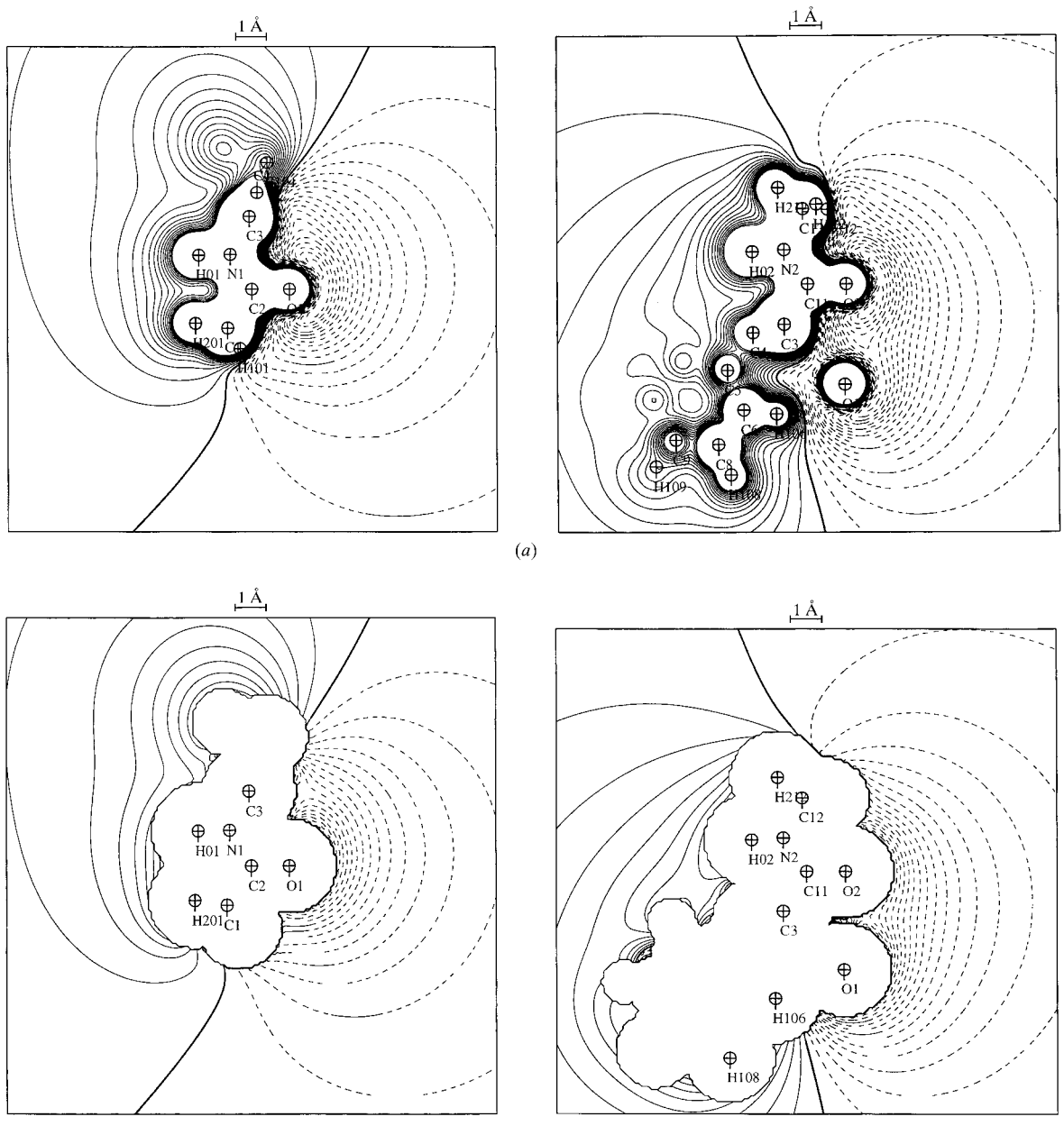

Fig. 7. Electrostatic potential maps of the two peptide links of *N*-acetyl-α,β-dehydrophenylalanine methylamide molecule: (*a*) experimental electrostatic potential; (*b*) up to hexadecapole level electric moments generated electrostatic potential. Same contours as in Fig. 2.

ited. Fig. 5 shows the maps of the resulting electrostatic potential for NAT and ASPA1 water molecules. The region close to the O_w nuclei is clearly better reproduced compared to Fig. 4. The difference maps between the generated potential with moments up to hexadecapole level and the observed electrostatic potential for ASPA1 and NAT water molecules have been deposited. The difference is almost zero in the intermolecular regions showing the excellent one-center electric moment representation of the experimental electrostatic potential.

4. Conclusions

Once the atomic moments are available from the fit of the electrostatic potential, the molecular or fragment electric moments can be analytically obtained by the Legendre polynomial translation method (Hobson, 1931). The electrostatic potential is expressed according to the Buckingham expansion with electric moments related to the molecular center of mass. These physical properties have been derived for the water molecule in the solid state. Furthermore, this method seems to be powerful even for systems as large as a 30-atom pseudopeptide molecule *N*-acetyl-α,β-dehydrophenylalanine methylamide (Souhassou *et al.*, 1992; Bouhmaida *et al.*, 1997) for which the six chosen fragments are represented in Fig. 6. Fig. 7 shows the excellent agreement between the observed (Fig. 7*a*) and fragment-moment-generated electrostatic potentials (Fig. 7*b*) in the planes of the two molecular peptide bonds outside the atomic van der Waals radii. Application of the method to fragments in large amino acid systems is in progress in order to reduce the number of centers for the electrostatic potential representation.

APPENDIX *A*
Cartesian expressions for the real spherical harmonic functions

Cartesian expressions for the real spherical harmonic functions used in this paper and their relation with the associated Legendre polynomials P_l^m [formula (3) in the text] are given below.

$y_{lm\pm}$	Cartesian form	$N_{lm}P_l^m \begin{cases} \cos m\varphi \\ \sin m\varphi \end{cases}$
y_{00}	1	P_0^0
y_{11+}	x	$P_1^1 \cos\varphi$
y_{11-}	y	$P_1^1 \sin\varphi$
y_{10}	z	P_1^0
y_{22+}	$x^2 - y^2$	$\frac{1}{3}P_2^2 \cos 2\varphi$
y_{22-}	xy	$\frac{1}{6}P_2^2 \sin 2\varphi$
y_{21+}	xz	$\frac{1}{3}P_2^1 \cos\varphi$
y_{21-}	yz	$\frac{1}{3}P_2^1 \sin\varphi$
y_{20}	$3z^2 - r^2$	$2P_2^0$
y_{33+}	$x^3 - 3xy^2$	$\frac{1}{15}P_3^3 \cos 3\varphi$
y_{33-}	$3yx^2 - y^3$	$\frac{1}{15}P_3^3 \sin 3\varphi$
y_{32+}	$(x^2 - y^2)z$	$\frac{1}{15}P_3^2 \cos 2\varphi$
y_{32-}	xyz	$\frac{1}{30}P_3^2 \sin 2\varphi$
y_{31+}	$(5z^2 - r^2)x$	$\frac{2}{3}P_3^1 \cos\varphi$
y_{31-}	$(5z^2 - r^2)y$	$\frac{2}{3}P_3^1 \sin\varphi$
y_{30}	$(5z^2 - 3r^2)z$	$2P_3^0$
y_{44+}	$x^4 - 6x^2y^2 + y^4$	$\frac{1}{105}P_4^4 \cos 4\varphi$
y_{44-}	$(x^2 - y^2)xy$	$\frac{1}{420}P_4^4 \sin 4\varphi$
y_{43+}	$(x^2 - 3y^2)xz$	$\frac{1}{105}P_4^3 \cos 3\varphi$
y_{43-}	$(3x^2 - y^2)yz$	$\frac{1}{105}P_4^3 \sin 3\varphi$
y_{42+}	$(7z^2 - r^2)(x^2 - y^2)$	$\frac{2}{15}P_4^2 \cos 2\varphi$
y_{42-}	$(7z^2 - r^2)xy$	$\frac{1}{15}P_4^2 \sin 2\varphi$
y_{41+}	$(7z^2 - 3r^2)xz$	$\frac{2}{5}P_4^1 \cos\varphi$
y_{41-}	$(7z^2 - 3r^2)yz$	$\frac{2}{5}P_4^1 \sin\varphi$
y_{40}	$7z^4 - 6z^2r^2 + (3/5)r^4$	$\frac{8}{5}P_4^0$

APPENDIX *B*
Relations between translated Q'_{lm} and Q_{lm} moments up to hexadecapole level

$$
\begin{aligned}
Q'_{10} &= Q_{10} - cQ_{00} \\
Q'_{11} &= Q_{11} \\
Q'_{1\bar{1}} &= Q_{1\bar{1}} \\
Q'_{20} &= Q_{20} - 2cQ_{10} + c^2Q_{00} \\
Q'_{21} &= Q_{21} - cQ_{11} \\
Q'_{2\bar{1}} &= Q_{2\bar{1}} - cQ_{1\bar{1}} \\
Q'_{22} &= Q_{22} \\
Q'_{2\bar{2}} &= Q_{2\bar{2}} \\
Q'_{30} &= Q_{30} - 3cQ_{20} + 3c^2Q_{10} - c^3Q_{00} \\
Q'_{31} &= Q_{31} - 2cQ_{21} + c^2Q_{11} \\
Q'_{3\bar{1}} &= Q_{3\bar{1}} - 2cQ_{2\bar{1}} + c^2Q_{1\bar{1}} \\
Q'_{32} &= Q_{32} - cQ_{22} \\
Q'_{3\bar{2}} &= Q_{3\bar{2}} - cQ_{2\bar{2}} \\
Q'_{33} &= Q_{33} \\
Q'_{3\bar{3}} &= Q_{3\bar{3}} \\
Q'_{40} &= Q_{40} - 4cQ_{30} + 6c^2Q_{20} - 4c^3Q_{10} + c^4Q_{00} \\
Q'_{41} &= Q_{41} - 3cQ_{31} + 3c^2Q_{21} - c^3Q_{11} \\
Q'_{4\bar{1}} &= Q_{4\bar{1}} - 3cQ_{3\bar{1}} + 3c^2Q_{2\bar{1}} - c^3Q_{1\bar{1}} \\
Q'_{42} &= Q_{42} - 2cQ_{32} + c^2Q_{22} \\
Q'_{4\bar{2}} &= Q_{4\bar{2}} - 2cQ_{3\bar{2}} + c^2Q_{2\bar{2}} \\
Q'_{43} &= Q_{43} - cQ_{33} \\
Q'_{4\bar{3}} &= Q_{4\bar{3}} - cQ_{3\bar{3}} \\
Q'_{44} &= Q_{44} \\
Q'_{4\bar{4}} &= Q_{4\bar{4}}
\end{aligned}
$$

APPENDIX *C*
Correspondence between hexadecapole traceless moments and Q_{4m}

The hexadecapole part $\mathbf{V}_H(\mathbf{r})$ of the electrostatic potential is then [as in formula (8)]

$$\begin{aligned}V_H(\mathbf{r}) = &[Q_{44}(x^4 - 6x^2y^2 + y^4) + Q_{4\bar{4}}(x^2 - y^2)xy \\ &+ Q_{43}(x^2 - 3y^2)xz + Q_{4\bar{3}}(3x^2 - y^2)yz] \\ &\times |\mathbf{r} - \mathbf{R}_g|^{-9} \\ &+ [Q_{42}(7z^2 - r^2)(x^2 - y^2) + Q_{4\bar{2}}(7z^2 - r^2)xy \\ &+ Q_{41}(7z^2 - 3r^2)xz + Q_{4\bar{1}}(7z^2 - 3r^2)yz] \\ &\times |\mathbf{r} - \mathbf{R}_g|^{-9} \\ &+ Q_{40}[7z^4 - 6z^2r^2 + (3/5)r^4]|\mathbf{r} - \mathbf{R}_g|^{-9},\end{aligned}$$

which can be formulated as

$$\begin{aligned}V_H(\mathbf{r}) = |\mathbf{r} - \mathbf{R}_g|^{-9}&[(Q_{44} - Q_{42} + \tfrac{3}{5}Q_{40})x^4 \\ &+ (Q_{44} + Q_{42} + \tfrac{3}{5}Q_{40})y^4 + (\tfrac{8}{5}Q_{40})z^4 \\ &+ (Q_{4\bar{4}} - Q_{4\bar{2}})x^3y + (-Q_{4\bar{4}} - Q_{4\bar{2}})y^3x \\ &+ (Q_{43} - 3Q_{41})x^3z + (-3Q_{43} - 3Q_{41})xy^2z \\ &+ (3Q_{4\bar{3}} - 3Q_{4\bar{1}})x^2yz + (-Q_{4\bar{3}} - 3Q_{4\bar{1}})y^3z \\ &+ (6Q_{42} - \tfrac{24}{5}Q_{40})x^2z^2 \\ &+ (-6Q_{44} + \tfrac{6}{5}Q_{40})x^2y^2 \\ &+ (-6Q_{42} - \tfrac{24}{5}Q_{40})y^2z^2 + (6Q_{4\bar{2}})xyz^2 \\ &+ (4Q_{4\bar{1}})yz^3 + (4Q_{41})xz^3].\end{aligned}$$

Therefore, the correspondence between the Buckingham hexadecapole traceless moments and the fitted Q_{4m} moments is

$$\begin{aligned}
\Phi_{xxxx} &= Q_{44} - Q_{42} + \tfrac{3}{5}Q_{40} & \Phi_{yyyx} &= -\tfrac{1}{4}(Q_{4\bar{4}} + Q_{4\bar{2}}) \\
\Phi_{zzzx} &= Q_{41} & \Phi_{xxxy} &= \tfrac{1}{4}(Q_{4\bar{4}} - Q_{4\bar{2}}) \\
\Phi_{yyyy} &= Q_{44} + Q_{42} + \tfrac{3}{5}Q_{40} & \Phi_{xxyy} &= -Q_{44} + \tfrac{1}{5}Q_{40} \\
\Phi_{xxzz} &= Q_{42} - \tfrac{4}{5}Q_{40} & \Phi_{yyzz} &= -Q_{42} - \tfrac{4}{5}Q_{40} \\
\Phi_{zzzz} &= \tfrac{8}{5}Q_{40} & \Phi_{xxyz} &= \tfrac{1}{4}(Q_{4\bar{3}} - Q_{4\bar{1}}) \\
\Phi_{yyyz} &= -\tfrac{1}{4}(Q_{4\bar{3}} + 3Q_{4\bar{1}}) & \Phi_{zzzy} &= Q_{4\bar{1}} \\
\Phi_{xyyz} &= -\tfrac{1}{4}(Q_{43} + Q_{41}) & \Phi_{xyzz} &= \tfrac{1}{2}Q_{4\bar{2}} \\
\Phi_{xxxz} &= \tfrac{1}{4}(Q_{43} - 3Q_{41}).
\end{aligned}$$

The support of the CNRS and the CNR (through grant no SPM/3375, 1998) is gratefully acknowledged. NB is grateful to the Université Henri Poincaré, Nancy 1 for 4 months of a 'Maître de Conférences invité' position.

References

Allen, F. (1986). *Acta Cryst.* B**42**, 512–522.

Bader, R. F. W. (1990). *Atoms in Molecules: a Quantum Theory*, pp. 13–52, 275–315. Oxford: Oxford Science Publications.

Bader, R. F. W. & Essen, H. (1984). *J. Chem. Phys.* **80**, 1943–1960.

Bader, R. F. W., MacDougall, P. J. & Lau, C. D. H. (1984). *J. Am. Chem. Soc.* **106**, 1594–1605.

Bouhmaida, N., Ghermani, N. E., Lecomte, C. & Thalal, A. (1997). *Acta Cryst.* A**53**, 556–563.

Buckingham, A. D. (1959). *Q. Rev. Chem. Soc.* **13**, 183–214.

Colonna, F., Angyan, J. G. & Tapia, O. (1990). *Chem. Phys. Lett.* **172**, 55–61.

Coppens, P. (1997). *X-ray Charge Densities and Chemical Bonding*. IUCr/Oxford University Press.

Coppens, P., Guru Row, T. N., Leung, P., Stevens, E. D., Becker, P. J. & Yang, Y. W. (1979). *Acta Cryst.* A**35**, 63–72.

Espinosa, E., Lecomte, C., Ghermani, N. E., Devémy, J., Rohmer, M. M., Bénard, M. & Molins, E. (1996). *J. Am. Chem. Soc.* **118**, 2501–2502.

Espinosa, E., Lecomte, C., Molins, E., Veintemillas, S., Cousson A. & Paulus, W. (1996). *Acta Cryst.* B**52**, 519–534.

Ghermani, N. E., Bouhmaida, N. & Lecomte, C. (1992–1998). *ELECTROS*98, *STATDENS*98: *Computer Programs to Calculate Electrostatic Properties from High-Resolution X-ray Diffraction.* Internal report UPRES A CNRS 7036, Université Henri Poincaré, Nancy 1, France.

Ghermani, N. E., Bouhmaida, N. & Lecomte, C. (1993). *Acta Cryst.* A**49**, 781–789.

Ghermani, N. E., Lecomte, C. & Bouhmaida, N. (1991). *Z. Naturforsch. Teil A*, **48**, 91–98.

Ghermani, N. E., Lecomte, C. & Dusausoy, Y. (1996). *Phys. Rev. B*, **53**, 5231–5239.

Hansen, N. K. & Coppens, P. (1978). *Acta Cryst.* A**34**, 909–921.

Hobson, E. W. (1931). *The Theory of Spherical and Ellipsoidal Harmonics*, pp. 136–141. Cambridge University Press.

Koch, U. & Egert, E. (1995). *J. Comput. Chem.* **16**, 937–944.

Lachekar, H. (1997). PhD thesis, Université Henri Poincaré, Nancy 1, France.

McLean A. D. & Yoshimine, M. (1967). *J. Chem. Phys.* **47**, 1927–1935.

Momany, F. A. (1978). *J. Phys. Chem.* **82**, 592–601.

Mulliken, R. S. (1955). *J. Chem. Phys.* **23**, 1833.

Pichon-Pesme, V., Lecomte, C., Wiest, R. & Bénard, M. (1994). *J. Am. Chem. Soc.* **98**, 1351–1362.

Price, S., Stone, A. J. & Alderton, M. (1984). *Mol. Phys.* **52**, 987–1001.

Souhassou, M., Lecomte, C., Ghermani, N. E., Rohmer, M. M., Wiest, R., Bénard, M. & Blessing, R. H. (1992). *J. Am. Chem. Soc.* **114**, 2371–2382.

Spackman, M. A. (1986). *J. Chem. Phys.* **85**, 6587–6601.

Spackman, M. A. (1992). *Chem. Rev.* **92**, 1769–1797.

Spackman, M. A. (1996). *J. Comput. Chem.* **17**, 1–18.

Woods, R. J., Khalil, M., Pell, W., Moffat, S. H. & Smith, V. H. (1990). *J. Comput. Chem.* **11**, 297–319.